



# DNA hybridization sensor based on pentacene thin film transistor<sup>☆</sup>

Jung-Min Kim<sup>a</sup>, Sandeep Kumar Jha<sup>a</sup>, Rohit Chand<sup>a</sup>, Dong-Hoon Lee<sup>a</sup>, Yong-Sang Kim<sup>a,b,\*</sup>

<sup>a</sup> Department of Nano Science & Engineering, Myongji University, Gyeonggi-do 449-728, Republic of Korea

<sup>b</sup> Department of Electrical Engineering, Myongji University, Gyeonggi-do 449-728, Republic of Korea

## ARTICLE INFO

### Article history:

Received 18 August 2010

Accepted 23 September 2010

Available online 1 October 2010

### Keywords:

Pentacene thin film transistors

DNA hybridization sensor

Disposable sensor

Label-free

## ABSTRACT

A DNA hybridization sensor using pentacene thin film transistors (TFTs) is an excellent candidate for disposable sensor applications due to their low-cost fabrication process and fast detection. We fabricated pentacene TFTs on glass substrate for the sensing of DNA hybridization. The ss-DNA (polyA/polyT) or ds-DNA (polyA/polyT hybrid) were immobilized directly on the surface of the pentacene, producing a dramatic change in the electrical properties of the devices. The electrical characteristics of devices were studied as a function of DNA immobilization, single-stranded vs. double-stranded DNA, DNA length and concentration. The TFT device was further tested for detection of  $\lambda$ -phage genomic DNA using probe hybridization. Based on these results, we propose that a “label-free” detection technique for DNA hybridization is possible through direct measurement of electrical properties of DNA-immobilized pentacene TFTs.

© 2010 Elsevier B.V. All rights reserved.

## 1. Introduction

Completion of Human genome project has necessitated rapid development in the field of nucleic acid diagnostics. The detection and quantification of DNA hybridization is also of great importance in many applications, such as medical diagnostics, forensic science, genotyping, and pathogen detection (Patolsky et al., 2001; Ramsay, 1998). Traditional methods for detection of DNA mainly focus on radio labeled system or optical detection using fluorochrome tagged oligonucleotides (Liu et al., 2009; Baselt et al., 1998). These detection techniques have limitations due to the complications in sample preparation as well as the necessary usage of complex and expensive optical systems, along with health risk. Compared with these techniques, label-free electronic methods promise to offer sensitivity, selectivity, and low cost for the detection of DNA hybridization. Recently, DNA hybridization sensors, using the “label-free” method, have been studied with much interest, including electrochemical detection (Cash et al., 2009), carbon nanotube network field-effect transistors (Tang et al., 2006), atomic force microscopy (AFM) (Wang and Bard, 2001), amperometry (Evtugyn et al., 2005), surface plasmon resonance (SPR) (Nelson et al., 2001), genetic field effect transistor (FET) (Estrale and Migliorato, 2007), and microcantilevers (McKendry et al., 2002). Among these methods, a DNA hybridization sensor using organic thin film transistors

(OTFTs) is an excellent candidate for the application as disposable sensors, due to their potentially low-cost fabrication process and quicker response time (Yan et al., 2009). Moreover, due to their biocompatibility and flexibility, an organic semiconductor material offers great opportunity for integration with biological systems.

For these reasons, in the present work, we fabricated organic TFTs using pentacene on glass substrates as a biosensor for DNA hybridization. Pentacene was the choice for the organic semiconductor material due to its excellent electrical properties and ease in immobilization of DNA on it. The target DNA was immobilized on the pentacene surface through physical adsorption without requiring any binding agents thereby reducing the use of reagents and fabrication cost. The adsorbed DNA on the OTFT attracts holes from channel region, causing a change in the resultant channel current and field-effect mobility during analysis. The magnitude of this change was significantly different for single stranded DNA (ss-DNA) and double stranded DNA (ds-DNA), thereby allowing us to sense the DNA hybridization.

## 2. Experimental

### 2.1. Materials

Poly(4-vinylphenol) (PVP), pentacene, ethidium bromide, propylene glycol methyl ether acetate, methylated poly(melamine-co-formaldehyde) and Eco-RI restriction-digested genomic DNA of lambda phage virus were purchased from Sigma Aldrich, Korea. Other chemicals and solvents were of analytical reagent grade and were used without further purification. The 25, 50 and 100 mer ss-DNA (polyA/polyT) or 25, 50 and 100 bp ds-DNA (polyA/polyT

<sup>☆</sup> The paper was presented at the World Congress on Biosensors 2010.

\* Corresponding author at: Department of Nano Science & Engineering, Myongji University, 38-2 Nam-dong Yongin, Gyeonggi 449-728, Republic of Korea. Tel.: +81 31 338 6327; fax: +81 31 321 0271.

E-mail address: [kys@mju.ac.kr](mailto:kys@mju.ac.kr) (Y.-S. Kim).

hybrid) molecules, 100 mer polyC and 20-mer probe against  $\lambda$ -phage genomic DNA used in this study were synthesized by Bionics Inc., Korea.

## 2.2. Methods

All solutions, including dilutions of DNA oligos were prepared in double-distilled deionized (DDI) water. The device characterization experiments were performed in at least triplicates otherwise indicated. The data analysis was carried out using Origin (v 7.5) software from Originlab.

### 2.2.1. Device fabrication

The pentacene TFT devices in this study were fabricated with the process illustrated in Fig. 1. The top-contact pentacene TFTs were fabricated on a glass substrate. An 80 nm thick Al gate electrode was first deposited on the glass surface by thermal evaporation. The gate insulator composed of poly(4-vinylphenol) (PVP) and was deposited over the Al gate electrode to a thickness of 480 nm by spin coating and subsequent baking at 200 °C for 1 h. The PVP solution was prepared by dissolving PVP (10 wt% of solvent) and methylated poly(melamine-co-formaldehyde) (5 wt% of solvent) as a cross-linking agent in propylene glycol methyl ether acetate solvent. The pentacene active layer was patterned through the shadow mask by thermal evaporation at a rate of 0.1 Å/s to a thickness of about 70 nm at a high vacuum ( $<5 \times 10^{-6}$  torr). The source and drain electrodes were made up of Au layer of 100 nm thickness, which were deposited by thermal evaporation using a shadow mask. The pentacene TFTs obtained had a channel length ( $L$ ) and width ( $W$ ) of 100 and 1000  $\mu\text{m}$ , respectively.

### 2.2.2. Immobilization of DNA on pentacene surface

The single stranded (ss) DNA was first immobilized by pipetting a 1- $\mu\text{l}$  drop of deionized (DDI) water containing the DNA onto the pentacene TFTs channel and then air-drying for 60 min. Subsequently, 1 ml of DDI water was dropped slowly through slant onto the TFT channel for thorough washing of surface. The devices were then air-dried for 60 min before being characterized at room temperature in ambient air using a Keithley 236 meter. The meter was interfaced with a computer using LabVIEW GPIB-software interface. Further, in order to validate DNA hybridization on same substrate, pentacene TFTs with immobilized ss-DNA (100 mer-polyA) were used for immobilization of complementary ss-DNA (100 mer-polyT for verification and poly-C as control). The devices were air-dried for 60 min, washed again with DDI water as before, and air-dried for 60 min before being characterized by Keithley 236 meter. Similarly, different length and concentrations of DNA oligos were used to determine their effect on device characteristics.

The fabricated device was also tested for detection and analysis of Eco-RI restriction-digested genomic DNA of lambda phage virus. For this purpose, a 20-mer 5'-GCA-AGT-ATC-GTT-TCC-ACC-GT-3' probe was immobilized on pentacene surface and characterized. Subsequently, the lambda phage DNA digest was preheated at 100 °C for 30 min to separate its strands and 1  $\mu\text{l}$  of this sample (to different concentration) was applied on probe-immobilized TFT surface. The devices were air-dried, washed with DDI water and used in further characterization as before.

### 2.2.3. Microscopic verification of DNA hybridization on same substrate

The immobilization of ss-DNA on the pentacene surface and subsequent hybridization of complementary strand was confirmed using fluorescent labeling of ds-DNA during hybridization process. The fluorescent intercalator ethidium bromide (EtBr) was used for this purpose. For control, pentacene channel of a device (without DNA immobilization) was labeled with EtBr. Other control device

was first immobilized with ss-polyA followed by treatment with EtBr solution (1  $\mu\text{l}$  of 0.1% W/V in DDI water). The DNA hybridization was verified with the device containing immobilized polyA, on which polyT was immobilized subsequently and allowed to interact with EtBr solution. The devices were washed with DDI water on each step. The fluorescent images of labeled DNA or control devices were obtained using a fluorescence microscope (Olympus BX50, Japan) with appropriate optical filters at excitation and emission wavelengths as 510–490 and 590 nm, respectively.

### 2.2.4. Characterization of the electrical performance of TFT devices

The performance of the pentacene TFT devices was measured in terms of their output and transfer characteristics. In order to find the output characteristics of devices, the channel current ( $I_{\text{DS}}$ ) was measured as a function of the drain-source voltage ( $V_{\text{DS}}$ ) under a constant gate voltage ( $V_{\text{GS}}$ ). Evaluation of transfer characteristics was carried by measuring the  $I_{\text{DS}}$  between the source and drain as a function of the  $V_{\text{GS}}$  under a constant  $V_{\text{DS}}$ . One of the important parameters of OTFT was the field-effect mobility of carriers in its channel region. The field-effect mobility ( $\mu_{\text{FET}}$ ) was determined using the saturation drain current ( $I_{\text{DS,sat}}$ ) which is given by

$$I_{\text{DS,sat}} = \frac{WC_{\text{PVP}}\mu_{\text{FET}}}{2L}(V_{\text{GS}} - V_{\text{TH}})^2 \quad (1)$$

where  $W$  is the width of the channel,  $L$  is the length of the channel,  $C_{\text{PVP}}$  is the capacitance per unit area of the PVP gate insulator,  $V_{\text{GS}}$  is the gate voltage and  $V_{\text{TH}}$  is the threshold voltage.

## 3. Results and discussion

### 3.1. Microscopic verification of DNA immobilization on pentacene surface

The immobilization and hybridization of DNA molecules on pentacene TFT surface was confirmed by fluorescence microscopy. Fig. 2(a) and (b) shows the bright field microscopic image of our device without and with immobilized ds-DNA, respectively. Fig. 2(c) shows fluorescent images of control device. For control, pentacene channel of a device (without DNA immobilization) was labeled with EtBr, which showed no fluorescence upon exposure. Another device was immobilized with ss-DNA polyA and further interacted with EtBr. As EtBr is an intercalating dye and binds only to the ds-DNA, therefore, device with immobilized ss-DNA did not show any fluorescence (Fig. 2(d)). Finally, ss-DNA polyT was hybridized on pentacene containing immobilized polyA and labeled with EtBr. Upon exposure, an orange red fluorescence characteristic to EtBr was seen (Fig. 2(e)) which confirms the immobilization and hybridization of DNA on the same pentacene TFT substrate.

### 3.2. Influence of binding of DNA on pentacene surface

The DNA molecules were immobilized on the hydrophobic pentacene surface by physical adsorption through their hydrophobic interactions. These molecules also have negatively charged phosphate groups on their backbone, which profoundly affects the electrical performance of the pentacene TFTs and can be regarded as the sole reason for using the pentacene TFTs for fabrication of DNA hybridization sensors. The DNA molecules were dissolved in DDI water rather than common buffers such as Tris, PBS, etc. The use of double distilled water throughout the study was to avoid interferences on the performance of pentacene TFTs by ionic species present in commonly used buffers. However, DDI water itself was expected to alter the electrical properties of TFTs. Therefore, it was first confirmed through control experiment in which only a drop of DDI water was added on pentacene TFT and air-dried. The device

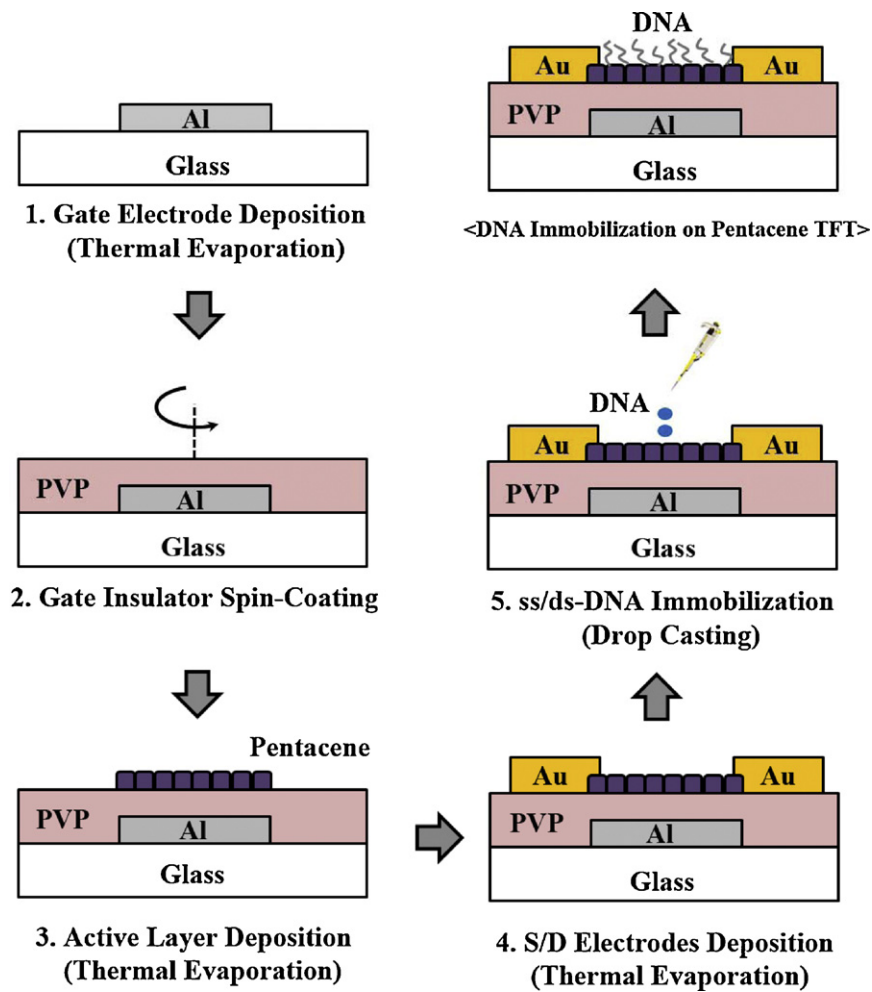


Fig. 1. Fabrication procedure of the pentacene TFTs and schematic of the DNA immobilization on pentacene TFTs.

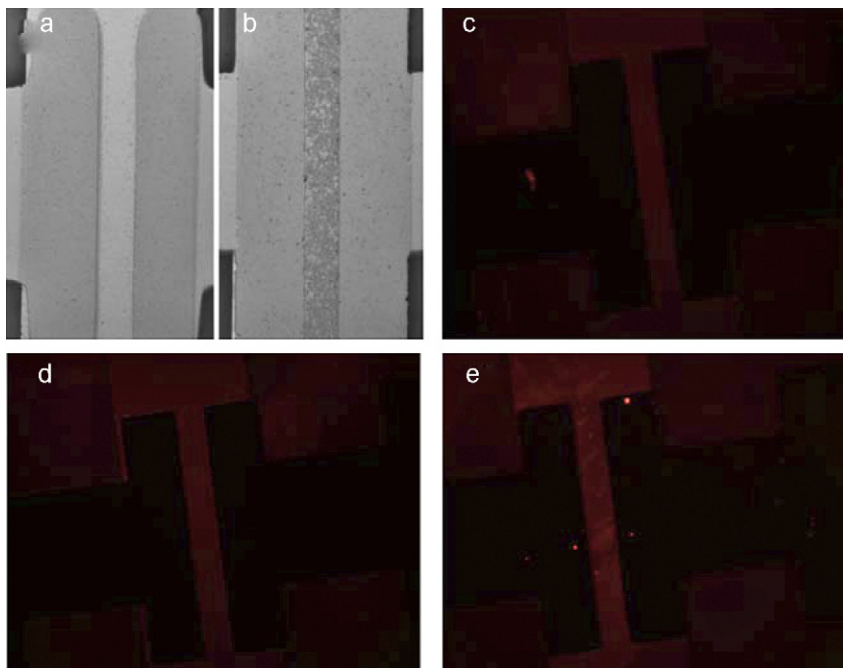
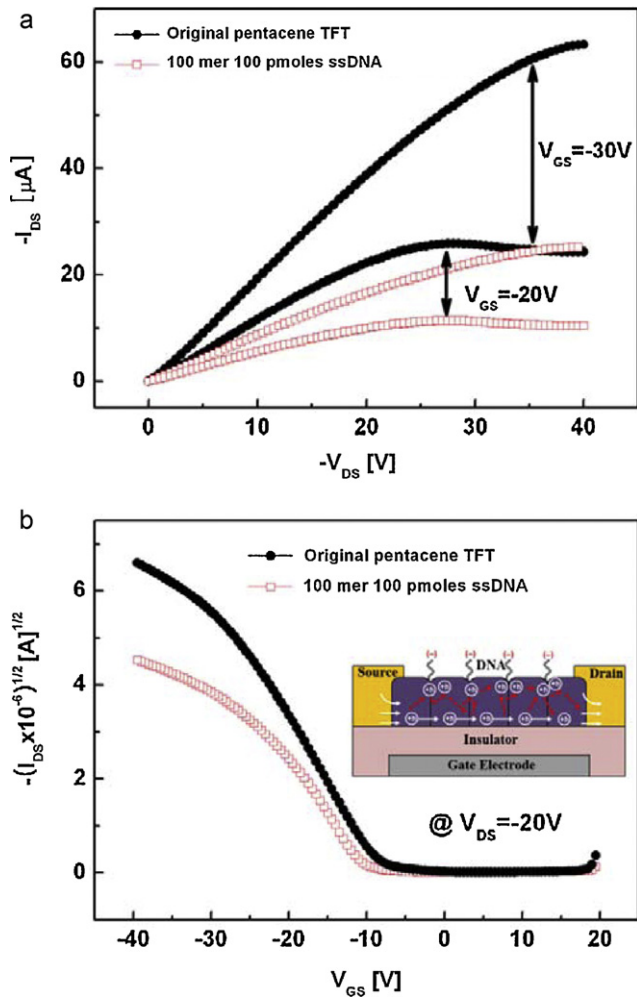


Fig. 2. Bright field microscopic pictures of pentacene TFTs without (a) and with (b) immobilized ds-DNA polyA-T, and fluorescence images of (c) pentacene TFT without DNA while labeled with EtBr, (d) pentacene TFT with ss-DNA labeled with EtBr and (e) pentacene TFT with ds-DNA, labeled with EtBr.



**Fig. 3.** Performance of the pentacene TFTs with DNA immobilized on pentacene: (a) output and (b) transfer characteristics of two pentacene TFTs (original, ss-DNA). The inset of shows the DNA sensing mechanism on the pentacene TFTs.

showed no alteration in the electrical properties of pentacene TFTs. On the other hand, pentacene TFTs showed reductions in channel current and field-effect mobility while analyzing DNA immobilized devices after rinsing with DDI water and air-drying for 1 h. Moreover, it is well known fact that adsorption of molecules on a surface is controlled through temperature and is governed by Freundlich isotherm curve. Therefore, all the studies were carried out at room temperature (25 °C in ambient air) to minimize variations in immobilization condition.

The influence of the immobilized DNA on pentacene surfaces was first studied by fabricating the pentacene TFTs with 100 mer, 100 pmol ss-DNA (polyA) for 60 min (immobilization time). Fig. 3(a) shows the  $I_{DS}$  as a function of  $V_{DS}$  under different  $V_{GS}$  (the output characteristic), whereas, Fig. 3(b) shows  $I_{DS}$  as a function of the  $V_{GS}$  measured at a constant  $V_{DS}$  (the transfer characteristic). At the same applied  $V_{GS}$ , original pentacene TFTs (without ss-DNA immobilization) showed higher  $I_{DS}$  than for pentacene TFTs with immobilized ss-DNA. After immobilizing ss-DNA, the  $I_{DS}$  of the device reduced approximately to 58.9% (at  $V_{DS} = -30V$ ,  $V_{GS} = -30V$ ). The field-effect mobility in the pentacene TFTs as given by Eq. (1) is influenced by the DNA molecules. Original pentacene TFTs have a field-effect mobility of  $\mu_{FET} = 1.81 \text{ cm}^2/\text{Vs}$ . Conversely, the pentacene TFTs with ss-DNA immobilization have a field-effect mobility of  $\mu_{FET} = 1.05 \text{ cm}^2/\text{Vs}$ . After immobilizing ss-DNA, field-effect mobility of the device reduced approximately to

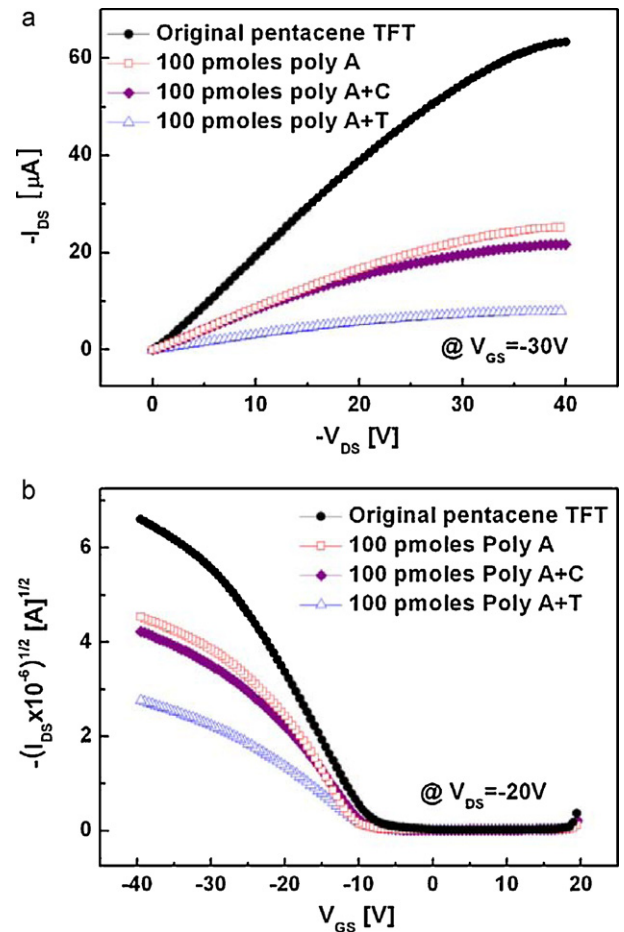


**Fig. 4.** Performance of the pentacene TFTs with DNA immobilized on same TFT surface: (a) output characteristics and (b) transfer characteristics of single pentacene TFTs as a function of different conditions (original device, polyA, polyC, polyT).

41.9%. The electrical characteristic of the pentacene TFTs with the ss-DNA immobilization gives a lower  $I_{DS}$  and field-effect mobility due to the DNA immobilization.

Such dramatic changes of electrical properties were well expected, since the phosphate group on the DNA backbone imparts a net negative charge in the DNA molecules, which attracts holes from the channel region, thereby decreasing the  $I_{DS}$  and field-effect mobility. The carrier collision or scattering affected the field-effect mobility in OTFT. The field-effect mobility of the hole is explained by equation

$$\mu_{FET} = \frac{v_{dp}}{E} = \frac{e\tau_{cp}}{m_p^*} \quad (2)$$

where  $v_{dp}$  is the average drift velocity of the holes,  $E$  is the electric field,  $e$  is the magnitude of the electronic charge,  $\tau_{cp}$  is a mean time between collisions or scattering and  $m_p^*$  is the effective mass of the hole.

There are two ways to study the change in electrical properties of pentacene TFTs. As shown in Fig. 3(a) and (b), the first figure shows output characteristics of TFTs that highlights transistor properties. Fig. 3(b) shows transfer characteristics of TFTs and can be used to calculate field-effect mobility and threshold voltage. The inset of Fig. 3(b) shows the DNA sensing mechanism of the pentacene TFTs. When the DNA molecules were immobilized on the pentacene surface, negative charge of DNA molecules attract holes from the channel region, thereby increasing the scattering of holes, while holes moves down from source to drain electrode. We expect the  $\tau_{cp}$  to decreases as the scattering increases, thus decreasing



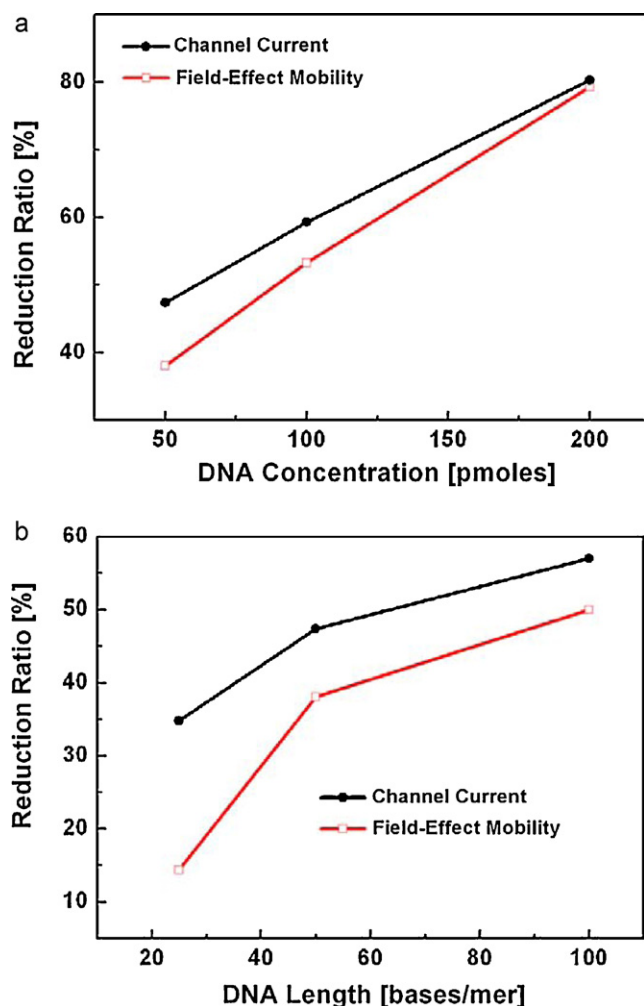


**Fig. 5.** Reduction ratio of channel current and field-effect mobility for the pentacene TFTs with immobilized ss-DNA, with respect to original device, as a function of DNA concentration (a) and DNA length (b).

field-effect mobility as calculated by Eq. (2). The  $I_{DS}$  of pentacene TFTs as given by Eq. (1) is influenced by the DNA molecules. The field-effect mobility decreases as the scattering of holes increases, thereby decreasing  $I_{DS}$ . This observation contradicts previous claim by Zang and Subramanian (2007) where the investigators reported an increase in  $I_{DS}$  level, which was a misinterpretation of current phenomena as we can show on the basis of present results.

Additionally, we also found a dramatic difference in the  $I_{DS}$  and pattern in field-effect mobility upon exposure to either 100 mer, 100 pmol ss-DNA or ds-DNA at same pentacene TFT. Fig. 4 shows the difference in the sensor output and the transfer characteristics from the original pentacene TFT (without ss-DNA) compared to the pentacene TFT with immobilized ss-DNA or ds-DNA. After immobilizing ds-DNA, the  $I_{DS}$  of the device reduced approximately to 86.55% compared with that of original device (at  $V_{DS} = -30$  V,  $V_{GS} = -30$  V) which was more than that for ss-DNA (58.9%). In addition, the field-effect mobility reduced to 41.9 and 84.41% for ss-DNA and ds-DNA, respectively. This enables the direct electrical detection of the DNA hybridization through the measurement of  $I_{DS}$  for the pentacene TFTs. The net difference in the  $I_{DS}$  ( $\Delta I_{DS}$ ) on the pentacene TFTs due to the single or double stranded DNA was the basis for the analysis of the DNA hybridization.

To confirm the DNA hybridization on single pentacene TFT, 100 pmol of 100 mer polyC was dropped on the polyA (100 mer, 100 pmol) immobilized pentacene TFT. In this device, polyC did

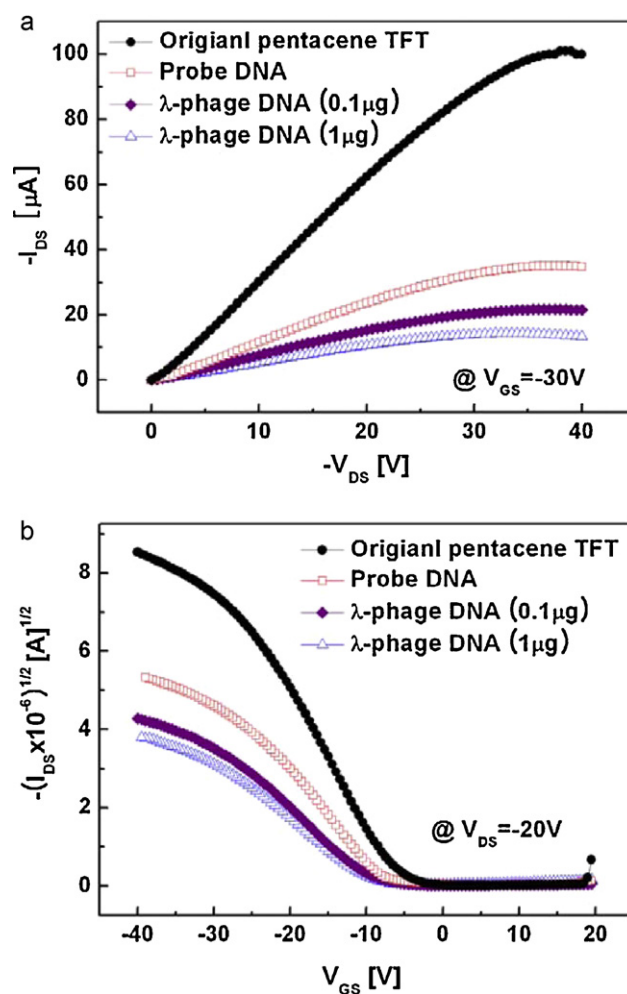


**Fig. 6.** Performance of the pentacene TFTs with single stranded 20-mer probe immobilized on pentacene surface and upon hybridization of  $\lambda$ -phage DNA. (a) Output characteristics and (b) transfer characteristics of three pentacene TFTs (original, ss-DNA, hybridized  $\lambda$ -phage DNA).

not immobilize on pentacene channel layer as polyA was already immobilized on this surface. Also, as expected, polyC did not hybridize to polyA. As a result, there was no significant alteration in the electrical properties of pentacene TFT (Fig. 4). On the other hand, the TFT device showed significant change in electrical properties due to hybridization by same concentration of polyT over polyA (Fig. 4). This result indicates the possibility of selective response from devices having different DNA molecules immobilized on pentacene.

In order to derive any correlation between the device response and the extent of the DNA concentration, the output and transfer characteristics of the devices were also measured by varying the concentration of the ss-DNA on the pentacene surface (Fig. 5(a)). As DNA concentration was increased, the  $I_{DS}$  value decreased approximately to 47.36, 59.31 and 80.35%, respectively and so a decrease in the field-effect mobility was observed which were approximately 38.06, 53.32 and 79.31%, respectively for 50, 100 and 200 pmol of 50-mer ss-DNA. Such a reduction in  $I_{DS}$  and field-effect mobility was due to the increase in the concentration of immobilized DNA on the pentacene surface, which collectively attracts more holes from the channel region. This result indicates the possibility of dynamic response from devices having low concentration of DNA immobilized on pentacene and enable estimation of DNA concentration upon hybridization.

As the length of ss-DNA immobilized on pentacene surface is also expected to influence the device properties, the output and transfer characteristics of the devices were measured while immobilizing varying length of ss-DNA on the pentacene surface. Fig. 5(b) shows the influence of the DNA length on pentacene surface, which was studied with 25, 50 and 100 mer ss-DNA of the same concentration (50 pmol). As DNA length was increased, the  $I_{DS}$  value decreased approximately to 34.8, 47.36 and 56.99% respectively and so a decrease in the field-effect mobility was observed to approximately 14.35, 38.06 and 50% level, respectively for 25, 50 and 100 mer DNA. Such a reduction in  $I_{DS}$  and field-effect mobility was due to the fact that longer DNA length carries more net negative charge.

Finally, as a proof of concept, we attempted to detect bacteriophage lambda through hybridization of genomic DNA of the virus over a probe-immobilized pentacene TFT device. For this purpose, a 20-mer probe 5'-GCA-AGT-ATC-GTT-TCC-ACC-GT-3' similar to the PCR primer used for amplification of organism's genomic DNA was immobilized on pentacene surface and characterized (Fig. 6). Subsequently, the lambda phage DNA digest was preheated at 100 °C for 30 min to separate its strands and 1 µl of this sample (containing 1 µg and 100 ng DNA) was applied on probe-immobilized TFT surface. Restriction digestion of lambda phage DNA ensured five smaller fragments of ds-DNA for ease in separating the strands and hybridization over its probe. The devices were air-dried, washed with DDI water and used in further characterization as before. As seen from Fig. 6, the device showed significant change in electrical properties on response to different concentrations of complementary DNA from λ-phage. This result demonstrates the feasibility of our device as a disposable sensor for DNA hybridization and can lead to development of biosensor for rapid pathogen detection.

#### 4. Conclusion

The single and double stranded DNA molecules were immobilized on the surface of the pentacene layer, producing a change

in the performance of the pentacene TFTs. It is attributable to the negative charges on the DNA molecules having the ability to attract holes from the channel region. The electrical characteristic of the pentacene TFTs with the ds-DNA immobilization gives a lower current output and field-effect mobility compared to ss-DNA since the ds-DNA carry more net negative charge. Therefore, we propose, in conclusion, that a “label-free” detection technique for DNA hybridization with high sensitivity and selectivity is possible to realize portable and disposable DNA sensor having application in molecular biology laboratories, medical diagnostics, forensic investigations, genotyping, pathogen detection and so on.

#### Acknowledgement

This work was supported by Grant no. (ROA-2006-000-10274-0) from the National Research Laboratory Program of the Korea Science & Engineering Foundation.

#### References

- Baselt, D.R., Lee, G.U., Natesan, M., Metzger, S.W., Sheehan, P.E., Colton, R.J., 1998. *Biosens. Bioelectron.* 13, 731–739.
- Cash, K.J., Heeger, A.J., Plaxco, K.W., Xiao, Y., 2009. *Anal. Chem.* 81, 656–661.
- Estrale, P., Migliorato, P., 2007. *J. Mater. Chem.* 17, 219–224.
- Evtugyn, G.A., Goldfarb, O.E., Budnikov, H.C., Ivanov, A.N., Vinter, V.G., 2005. *Sensors* 5, 364–376.
- Liu, J., Cao, Z., Lu, Y., 2009. *Chem. Rev.* 109, 1948–1998.
- McKendry, R., Zhang, J.Y., Arntz, Y., Strunz, T., Hegner, M., Lang, H.P., Baller, M.K., Certa, U., Meyer, E., Guntherodt, H.J., Gerber, C., 2002. *Proc. Natl. Acad. Sci. U.S.A.* 99, 9783–9788.
- Nelson, B.P., Grimsrud, T.E., Liles, M.R., Goodman, R.M., Corn, R.M., 2001. *Anal. Chem.* 73, 1–7.
- Patolsky, F., Lichtenstein, A., Willner, I., 2001. *Nat. Biotechnol.* 19, 253–257.
- Ramsay, G., 1998. *Nat. Biotechnol.* 16, 40–44.
- Tang, X., Bansaruntip, S., Nakayama, N., Yenilmez, E., Chang, Y.L., Wang, Q., 2006. *Nano Lett.* 6, 1632–1636.
- Wang, J., Bard, A., 2001. *J. Anal. Chem.* 73, 2207–2212.
- Yan, F., Mok, S.M., Yu, J., Chan, H.L.W., Yang, M., 2009. *Biosens. Bioelectron.* 24, 1241–1245.
- Zang, Q.T., Subramanian, V., 2007. *Biosens. Bioelectron.* 22, 3182–3187.